

Synthesis and Studying the Morphological and Some Optical Properties of Iron Oxide Under Influence of Annealing time

Shaymaa. A. Mukheef , Fouad Sh. Hashim , Khalid Haneen Abass

Department of Physics, College of Education for Pure Sciences, University of Babylon, Iraq

Abstract

In this research, iron nanofilm deposited by thermal evaporation method on glass substrate were annealed at 200 °C for 2, 3 and 4 hours to obtain Iron Oxide films. Atomic force microscopy (AFM) confirmed that the films grown had a good homogeneous surface. The roughness, root mean square value, and the average diameter increased with the increasing of annealing time. The absorbance of the films were recorded using UV-Visible spectrophotometer. The absorbance increased at UV region and then decreased with the increasing annealing time at visible and near infrared region, while the transmittance decrease at UV region and then increase with increasing annealing time at visible and near infrared region. The direct energy gap decreased from 3.48 eV for as-deposited film to 3.33eV at 200 °C for 4 hours. The absorption coefficient, extinction coefficient and refractive index decreased with increasing annealing time.

Keywords: Iron oxide, annealing time, nanoparticle, AFM, optical properties.

1.Introduction

Over the last two decades, there has been a growing interest in many regions of research areas in the field of nanoscale materials that could be obtained using various techniques, including physical and chemical methods [1,2]. Due to various their small size (diameters tend to range from 1 to 100 nm), nanoparticles have unique and controllable characteristics that differ from some of those found on the macro scale, allowing for novel applications [3-8]. From among different kinds of nanomaterials, magnetic iron oxides (Fe_2O_3) exist in four crystalline polymorphs, each with a different crystalline structure that controls their physical characteristics. Due to their numerous technological applications, such as magnetic devices, sensors, lithium ion batteries, pigment, electrode material, magnetic materials, and photovoltaic devices, Fe_2O_3 is the most popular and promising material [9-15]. Magnetic iron oxide nanoparticles were created using a variety of techniques, including co-precipitation of ferrous/ferric salts [16], thermal degradation of hydrazinated iron(II) oxalate [17], microemulsion [18], sol-gel syntheses [19], and hydroxylation and pyrosol [20]. The current work deals with the synthesis of iron oxide nanofilms from Iron nanoparticles and the study of their morphological and some optical properties under influence of annealing time.

2. Experimental

2.1 Purification of iron oxide nanofilms

Thermal evaporation system (Edward C-306) was used to prepare iron nanofilms deposited on glass substrate. As source materials for the molybdenum boat, 99.9% pure iron powder was used. The chamber was evacuated to a pressure of 10^{-6} mbar. The distance between the source and the substrate was approximately 15 cm, and the nanofilms were annealed at 200 °C for 2, 3, and 4 hours, respectively.

2.2 Descriptions

The Atomic Force Microscope (AFM type (Aa3000 SPM)) was used to recognize the surface topography of the deposited iron oxide nanofilms. The UV-Visible spectrophotometer (Shimadzu UV1650 PC, Phillips, Japanese company) was considered, to record the transmission in the range of the wavelength (190-1100) nm at RT.

3. Results and Discussion

The typical AFM scans of the prepared iron oxide nanofilms as deposited and different annealing time in air at 200 °C for 2, 3 and 4 hours, are presented in Figs.(1-4) . The AFM images of iron oxide films show a high surface homogeneity in which the distribution of crystalline granules is uniform which is evident from the convergence of the roughness and root mean square (RMS) values as in Table(1). The white areas of the images indicate that there are set of crystalline granules one on top other, so it can be believe that the adjacent granules come together to form large clusters; therefore, we find that the granules in the white areas are larger than that in other regions. The roughness and root mean square (RMS) values are increased from 1.1 nm and 1.43 nm as-deposited nanofilm to 8.35 nm and 10.6 nm annealed at 200 °C for 3 hours, which is attributed to the fact that the surface diffusion was sufficient due to the deposition temperature. The increase in RMS lead to increase in crystalline growth in vertical direction more than horizontal direction. Similar behavior was reported in [21].

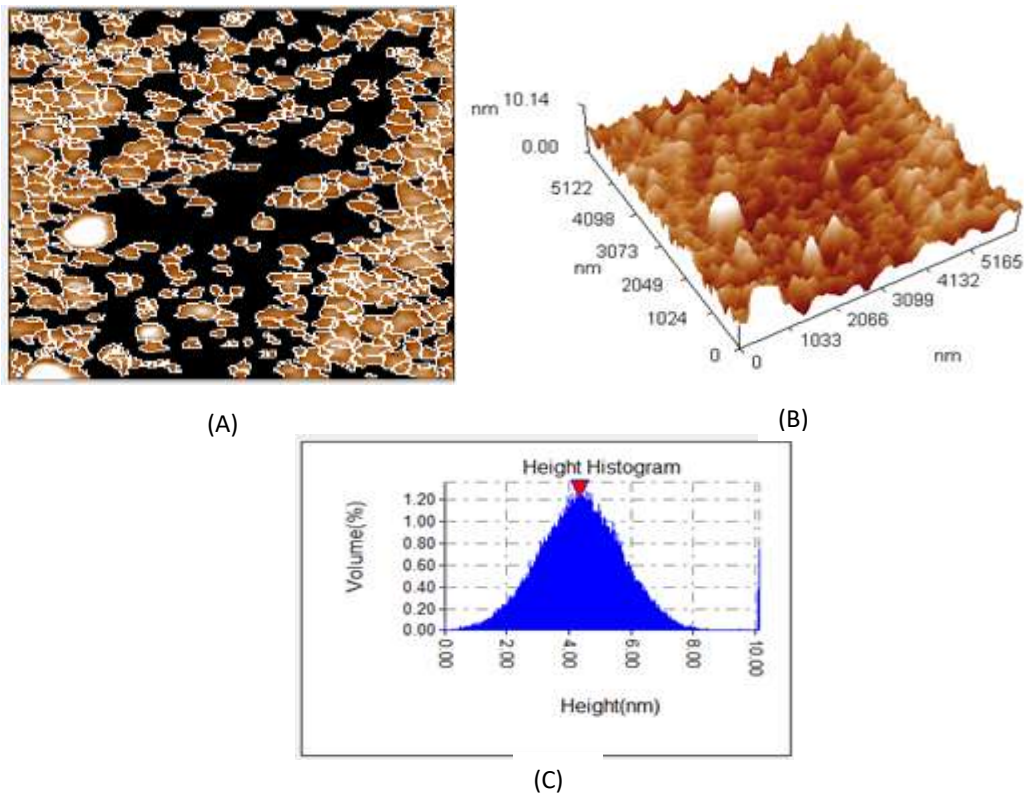


Fig.(1): AFM images of iron oxide nanofilm as-deposited for A) Histogram grain B) 3D and C) Height distribution with data report

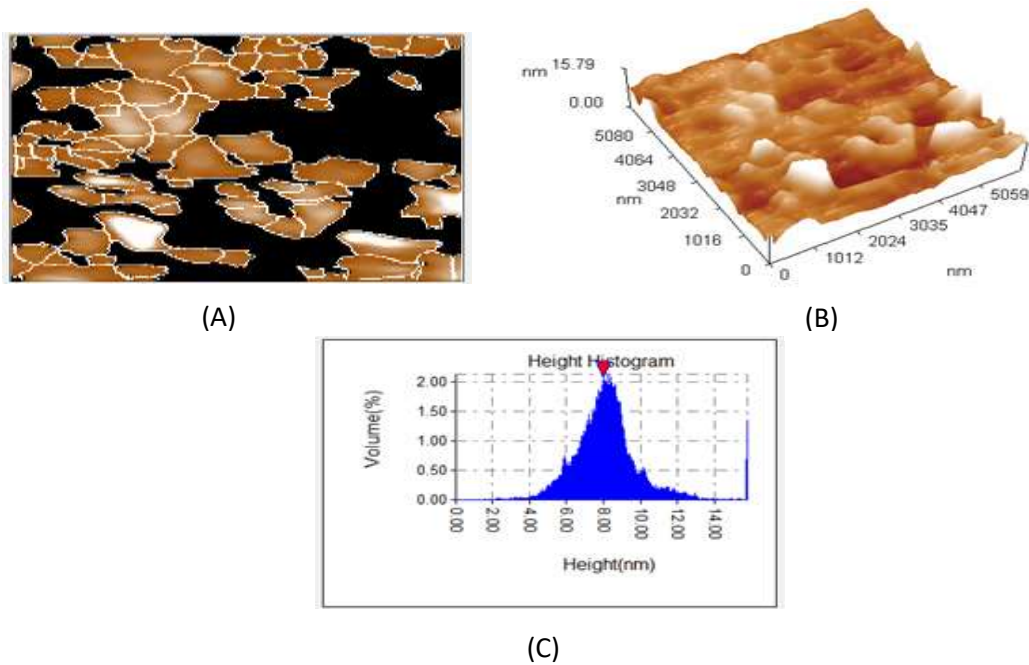
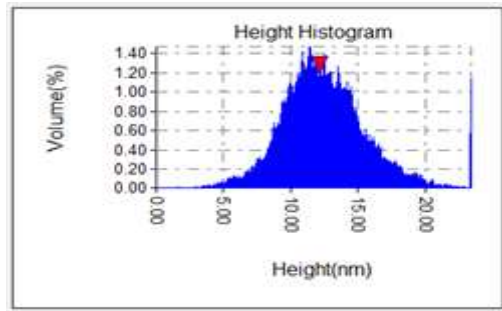
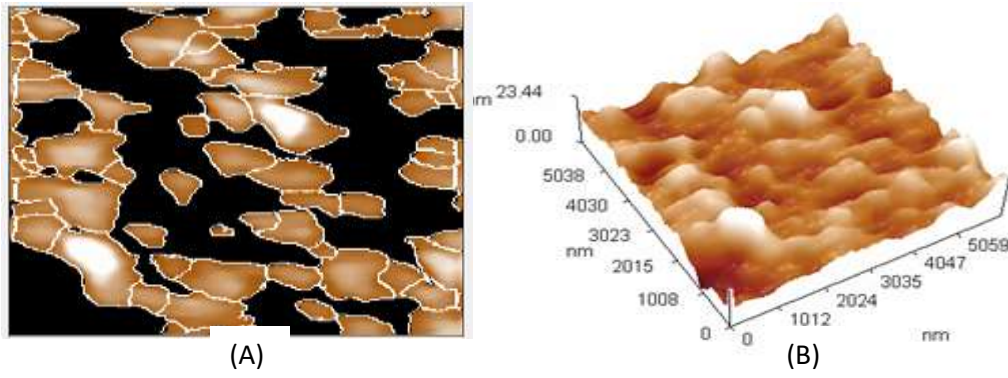
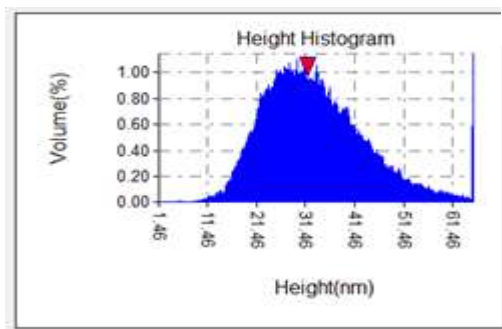
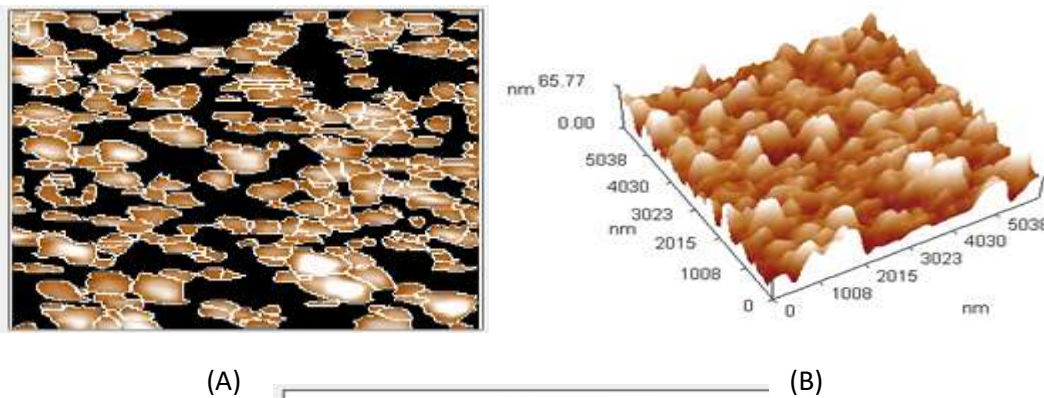


Fig.(2): AFM images of iron oxide nanofilm at 200°C for 2 hours for A) Histogram grain B) 3D and C) Height distribution with data report



(C)

Fig.(3): AFM images of iron oxide nanofilm at 200°C for 3 hours for A) Histogram grain B) 3D and C) Height distribution with data report



(C)

Fig.(3): AFM images of iron oxide nanofilm at 200°C for 4 hours for A) Histogram grain B) 3D and C) Height distribution with data report

Table (1): AFM of iron oxide with different Annealing Time

Annealing time (h)	Roughness average (nm)	Root mean square (nm)	Ten point height (nm)	Average Diameter(nm)
as-deposited	1.1	1.43	8.74	201.9
2	1.33	1.91	10.1	499
3	2.49	3.25	14.5	542.4
4	8.35	10.6	63.2	276.7

The absorbance and transmittance spectra of deposited Fe nanofilm and annealed at 200 °C for 2, 3, and 4 hours as a function of wavelength are shown in Figs.(5,6). The absorbance (Fig. 5) increases with increasing annealing time in the UV region and then reduces with increasing annealing time in the visible and NIR regions, whereas the transmittance (Fig. 6) reduces with increasing annealing time in the UV region and then increases with increasing annealing time in the visible and NIR regions. This behavior was attributed to a decrease in Fe content caused by an increase in the rate of re-evaporation of Fe atoms from the iron oxide film. This result is consistent with the findings of the researcher [22].

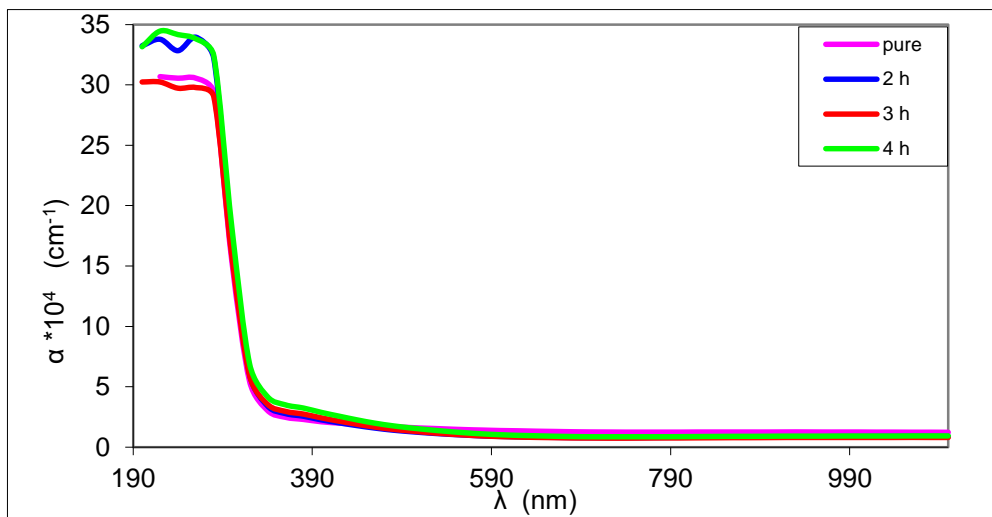


Fig.(4) Absorption coefficient of iron oxide film with different Annealing Time.

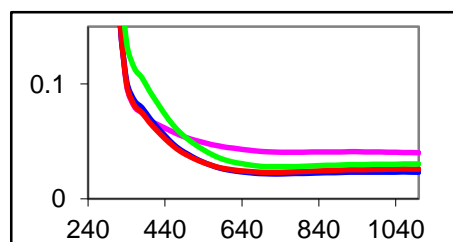


Fig. (5) Absorbance spectra of iron oxide nanofilm with different annealing time

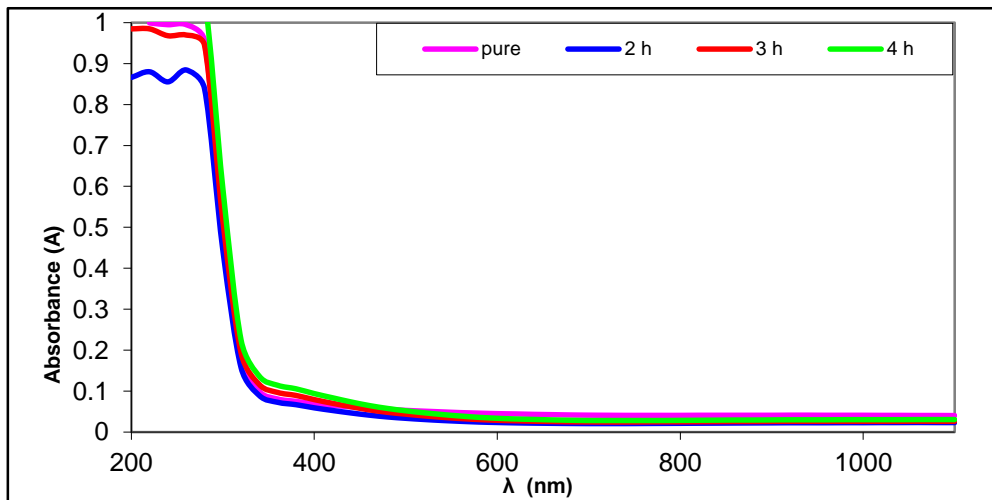


Fig. (6) Transmittance spectra of iron oxide nanofilm with different annealing time.

The absorption coefficient (α) has been calculated from the following equation [23].

$$\alpha = 2.303 (A/d) \quad (1)$$

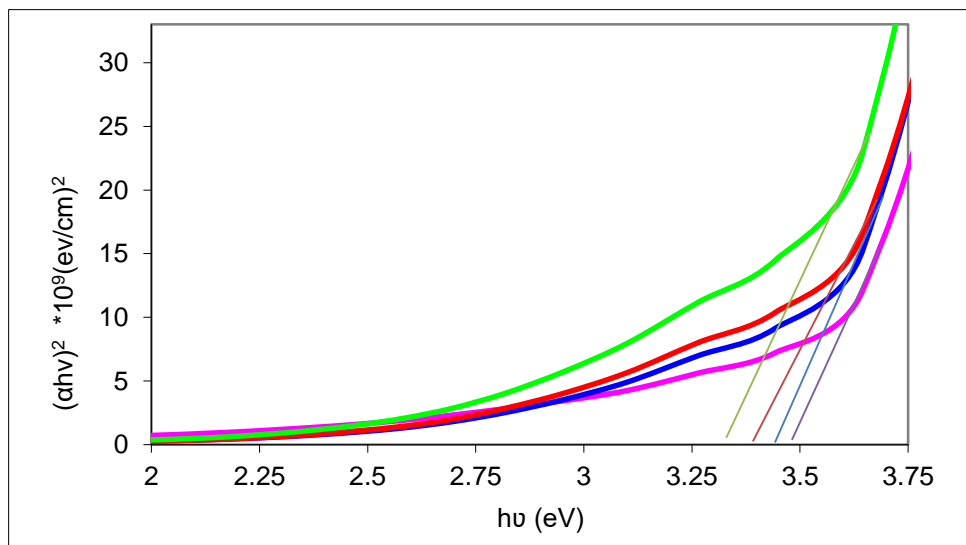
where: A is the absorbance and d is the thickness.

Fig.(7) show that the absorption coefficient of deposited Fe nanofilm and annealed at 200 °C for 2, 3, and 4 hours as a function of wavelength respectively. The absorption coefficient given the information on the transition nature. The value of α is greater than 10^4 cm^{-1} which mean the direct electron transition happen.

The direct optical energy gap (E_g^{opt}) of iron oxide nanofilms was calculated from equation [24,25]:

$$(\alpha h\nu)^2 \approx h\nu - E_g \quad (2)$$

Figure (8) obtain the E_g^{opt} as-deposited and different annealing time. The plot of $(\alpha h\nu)^2$ against $h\nu$ is linear in nature, indicating that the material of the nanofilms has a direct E_g^{opt} . The extrapolation of the straight line to $\alpha=0$ gives a direct E_g^{opt} equal to 3.48 eV for the as-deposited nanofilms and this value reduce with increasing annealing time and takes the values 3.45, 3.39 and 3.33 eV at 2, 3 and 4 hours respectively, which is agree with report [26, 27].



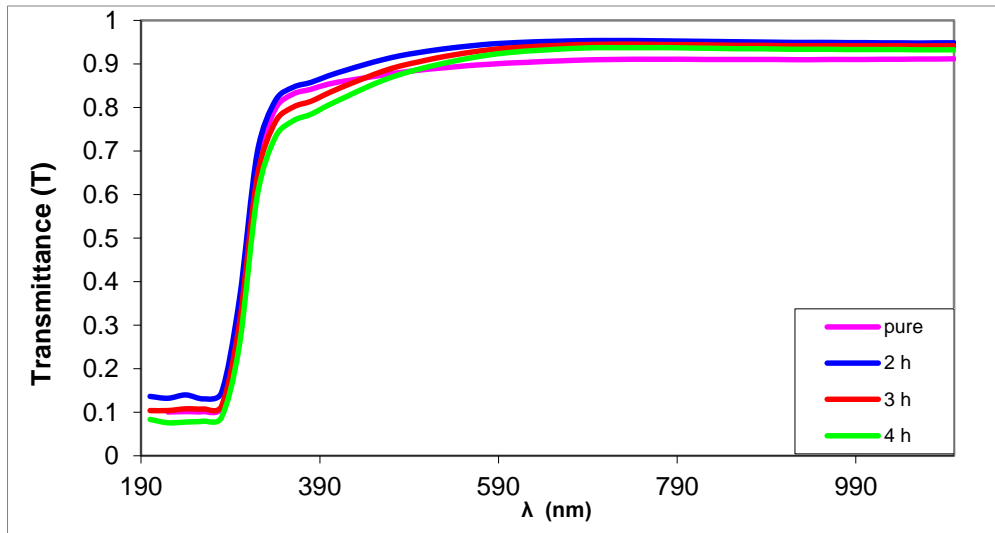


Fig.(8) The direct band gap of iron oxide nanofilm with different annealing time.

The extinction coefficient (k) and refractive index (n) has been calculated from equations [28,29]:

$$k = \frac{\alpha\lambda}{4\pi} \quad (3)$$

wherever λ is the wavelength.

Defines the refractive index (n) [30,31]:

$$n = \left(\frac{4R}{(R-1)^2} - k^2 \right)^{1/2} + \frac{(R+1)}{(R-1)} \quad (4)$$

at which R denotes reflection

From the Fig. (9,10), it was found that k and n decrease with increasing annealing time in the visible and NIR regions. This behavior is explained by the fact that the k has a similar behavior to the absorption coefficient according to equation (3) and the decrease in refractive index is explained by the decrease in density of nanofilms with increasing annealing time.

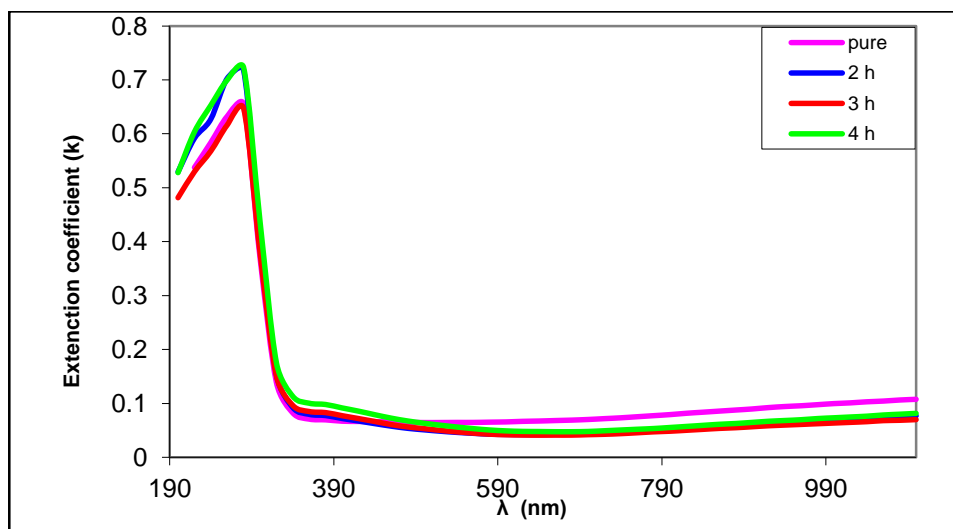


Fig.(6) Extinction coefficient of iron oxide nanofilm with different annealing time.

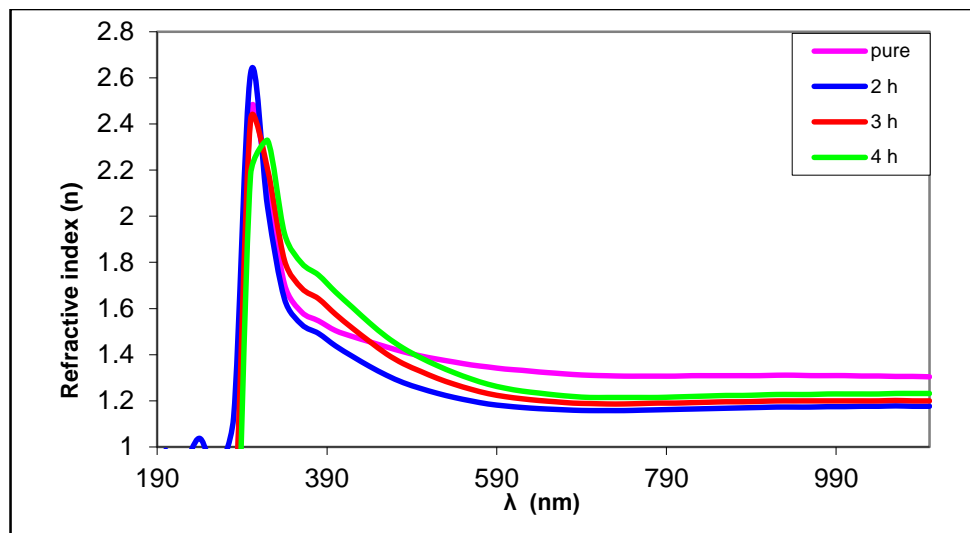


Fig.(7) Refractive index of iron oxide nanofilm with different annealing Time.

4. Conclusion

In summary, thermal evaporation technique was successfully to prepare iron oxide nanofilms using various annealing time after thermally preparation of iron films. AFM established that the films grown by this technique had a good homogeneous surface. The roughness, and root mean square value, increased with the increasing of annealing time. The optical characteristic include absorbance increase at UV region and then decrease with increasing annealing time at visible and NIR regions, while the transmittance decrease at UV region and increase with increasing annealing time at visible and NIR regions. The direct energy gap, absorption coefficient, extinction coefficient and refractive index decrease with increasing annealing time.

References

- [1] Machala L, Tucek J, Zboril R (2011) Polymorphous transformations of nanometric iron (III) oxide: a review. *Chem Mater* 23(14):3255-3272.
- [2] Hanan H. Jassim , Fouad Sh. Hashim, "Synthesis of (PVA/PEG: ZnO and Co₃O₄) Nanocomposites: Characterization and Gamma Ray Studies," *J. NeuroQuantology*, vol. 19, no. 4, 47-56, (2021) .
- [3] Srivastava M, Chaubey A, Ojha AK (2009) Investigation on size dependent structural and magnetic behavior of nickel ferrite nanoparticles prepared by sol-gel and hydrothermal methods. *Mater Chem Phys* 118(1):174-180.
- [4] Abass, K.H., Shinen, M.H., Alkaim, A.F., "Preparation of TiO₂ nanolayers via. sol-gel method and study the optoelectronic properties as solar cell applications", *Journal of Engineering and Applied Sciences*, 13(22), pp. 9631-9637, 2018.
- [5] Abass, K.H., Adil, A., Mohammed, M.K., "Fabrication and enhancement of SnS:Ag/Si solar cell via. thermal evaporation technique", *Journal of Engineering and Applied Sciences*, 13(4), pp. 919-925, 2018.
- [6] Haneen Abass, K., Haidar Obaid, N., "0.006wt.% Ag-Doped Sb₂O₃ Nanofilms with Various Thickness: Morphological and optical properties", *Journal of Physics: Conference Series*, 1294(2), 2019.
- [7] Tuama, A.N., Abbas, K.H., Hamzah, M.Q., Mezan, S.O., Jabbar, A.H., Agam, M.A., "An overview on characterization of silver/cuprous oxide nanometallic (Ag/Cu₂O) as visible light photocatalytic", *International Journal of Advanced Science and Technology*, 29(3), pp. 5008-5018, 2020.
- [8] Khalid Haneen Abass, Ashraq Mohammed Kadim, Sara Kareem Mohammed, Mohd Arif Agam, "Drug Delivery Systems Based on Polymeric Blend: A Review", *Nano Biomed. Eng.*, 2021, Vol. 13(4), p414-424.
- [9] N. Song, H. Jiang, T. Cui, L. Chang, X. Wang, Synthesis and enhanced gas-sensing properties of mesoporous hierarchical α -Fe₂O₃ architectures from an eggshell membrane, in: *Micro & Nano Letters*, Institution of Engineering and Technology, 2012; pp. 943-946
- [10] M. Mohapatra, D. Behera, S. Layek, S. Anand, H.C. Verma, B.K. Mishra, Influence of Ca Ions on Surfactant Directed Nucleation and Growth of Nano Structured Iron Oxides and Their Magnetic Properties, *Crystal Growth & Design*, 12 (2012) 18-28.
- [11] Q.A. Pankhurst, J. Connolly, S.K. Jones, J. Dobson, Applications of magnetic nanoparticles in biomedicine, *Journal of Physics D: Applied Physics*, 36 (2003) R167
- [12] T. Sugimoto, A. Muramatsu, K. Sakata, D. Shindo, Characterization of Hematite Particles of Different Shapes, *Journal of Colloid and Interface Science*, 158 (1993) 420-428.

- [13] A.S. Teja, P.-Y. Koh, Synthesis, properties and applications of magnetic iron oxide nanoparticles, *Progress in Crystal Growth and Characterization of Materials*, 55 (2009) 22-45.
- [14] L. Wang, L. Gao, Morphology Transformation of Hematite Nanoparticles Through Oriented Aggregation, *Journal of the American Ceramic Society*, 91 (2008) 3391-3395.
- [15] P. Gangopadhyay, S. Gallet, E. Franz, A. Persoons, T. Verbiest, Novel superparamagnetic Core (Shell) nanoparticles for magnetic targeted drug delivery and hyperthermia treatment, *IEEE Transactions on Magnetics*, 41 (2005) 4194-4196.
- [16] A. Jafari, S. F. Shayesteh, M. Salouti, and K. Boustani, "Effect of annealing temperature on magnetic phase transition in Fe₃O₄ nanoparticles," *Journal of Magnetism and Magnetic Materials*, vol. 379, pp. 305–312, 2015.
- [17] K. S. Rane and V. M. S. Verenkar, "Synthesis of ferrite grade γ -Fe₂O₃," *Bulletin of Materials Science*, vol. 24, No. 1, pp. 39–45, 2001.
- [18] A. B. Chin and I. I. Yaacob, "Synthesis and characterization of magnetic iron oxide nanoparticles via w/o microemulsion and Massart's procedure," *Journal of Materials Processing Technology*, vol. 191, no. 1–3, pp. 235–237, 2007.
- [19] K. Woo, H. J. Lee, J.-P. Ahn, and Y. S. Park, "Sol-gel mediated synthesis of Fe₂O₃ nanorods," *Advanced Materials*, vol. 15, no. 20, pp. 1761–1764, 2003.
- [20] E. Herrero, M. V. Cabañas, M. Vallet-Regí, J. L. Martínez, and J. M. González-Calbet, "Influence of synthesis conditions on the γ -Fe₂O₃ properties," *Solid State Ionics*, vol. 101–103, no. 1, pp. 213–219, 1997.
- [21] Alaa Nihad Tuama, Khalid Haneen Abass, Mohd Arif Agam, "Fabrication and Characterization of Cu₂O:Ag/Si Solar Cell Via Thermal Evaporation Technique", *International Journal of Nanoelectronics and Materials* Vol. 13, No. 3, p.p 601-614, 2020.
- [22] Abass, K. H., & Mohammed, M. K., "Fabrication of ZnO: Al/Si solar cell and enhancement its efficiency via Al-doping" *Nano Biomed. Eng*, 11(2), 170-177, 2019.
- [23] Esraa H. Hadi, Dhay Ali Sabur, Sami Salman Chiad, Nadir Fadhil Habubi, Khalid Haneen Abass, "Physical Properties of Nanostructured Li-Doped ZrO₂ Thin Films", *Journal of Green Engineering*, Vol.10, Issue-10, p.p 8390-8400, 2020.
- [24] J. Tauc, A. Menth, D. Wood, *Phys. Rev. Lett.* 25 (1970) 749–752.
- [25] Tuama, A.N., Abass, K.H., Bin Agam, M.A., "Efficiency enhancement of nano structured Cu₂O:Ag/ laser etched silicon-thin films fabricated via vacuum thermal evaporation technique for solar cell application", *Optik*, 2021, 247, 167980.
- [26] Kumar, Ajay, and Kamlesh Yadav. "Optical properties of nanocrystallite films of α -Fe₂O₃ and α -Fe_{2-x}Cr_xO₃(0.0≤x≤0.9) deposited on glass substrates " *Materials Research Express* 4.7, (2017).
- [27] B. Ouertani, J. Ouerfelli, M. Saadoun, H. Ezzaouia, B. Bessaïs, *Thin Solid Films* 516(23), 8584 (2008).
- [28] Akhavan, Omid. "Thickness dependent activity of nanostructured TiO₂/ α -Fe₂O₃ photocatalyst nanofilms." *Applied Surface Science* 257.5 (2010): 1724-1728.
- [29] Sakhil, M.D., Shaban, Z.M., Sharba, K.S., Habub, N.F., Abass, K.H., Chiad, S.S., Alkelaby, A.S., "Influence MgO dopant on structural and optical properties of nanostructured CuO thin films", *NeuroQuantology*, 18(5), pp. 56-61, 2020.
- [30] Ferdous, Zannatul, Md Samir Ullah, and Sabina Hussain, "Temperature and Substrate Effects on the Structural, Morphological, and Optical Properties of Iron Oxide Nanofilms Prepared by Spray Pyrolysis Technique." *Dhaka University Journal of Science* 68.1 (2020): 79-85.
- [31] Muhammad, S.K., Taqi, N.D.M., Chiad, S.S., Abass, K.H., Habubi, N.F., "Influence of nanostructured nio thin films doped with chrome by using green chemical spray gyrolysis csp", *Journal of Green Engineering*, 11(2), pp. 1287-1299, 2021.